A Framework for the Design & Operation of a Large-Scale Wind-Powered Hydrogen Electrolyzer Hub

Nathanial Cooper[1*], Christian Horend[1,2], Fritz Röben[3], Andre Bardow[4], Nilay Shah[1]

[1] Centre for Process Systems Engineering, Chemical Engineering, Imperial College London, Exhibition Road, London, UK
[2] Institute of Technical Thermodynamics, RWTH Aachen University, 52056 Aachen, Germany
[3] Institute of Energy and Climate Research IEK-10, Forschungszentrum Jülich GmbH, 52425 Jülich, Germany
[4] Energy and Process Systems Engineering, ETH Zurich, Zurich, Switzerland
* Corresponding Author: nathanial.cooper@imperial.ac.uk

Abstract

Due to the threat of climate change, renewable feedstocks & alternative energy carriers are becoming more necessary than ever. One key vector is hydrogen, which can fulfil these roles and is a renewable resource when split from water using renewable electricity. Electrolyzers are often not designed for variable operation, such as power from sources like wind or solar. This work develops a framework to optimize the design and operation of a large-scale electrolyzer hub under variable power supply. The framework is a two-part optimization, where designs of repeated, modular units are optimized, then the entire system is optimized based on those modular units. The framework is tested using a case study of an electrolyzer hub powered by a Dutch wind farm to minimize the levelized cost of hydrogen. To understand how the optimal design changes, three power profiles are examined, including a steady power supply, a representative wind farm power supply, and the same wind farm power supply compressed in time. The work finds the compressed power profile uses PEM technology which can ramp up and down more quickly. The framework determines for this case study, pressurized alkaline electrolyzers with large stacks are the cheapest modular unit, and while a steady power profile resulted in the cheapest hydrogen, costing 4.73 €/kg, the typical wind power profile only raised the levelized cost by 2% to 4.82 €/kg. This framework is useful for designing large-scale electrolysis plants and understanding the impact of specific design choices on the performance of a plant.

Keywords: electrolysis; hydrogen; wind power; levelized cost of hydrogen; economic optimization; Mixed Integer Linear Program

Nomenclature

A_0	base stack area for a reference stack
A_{stack}	stack area
A_{surf}	estimated surface area of the electrolyzer stack
$AE(t,e)$	available electricity at any time in any price tier (MW)
AF	annualization factor
$blockCap(k,l,m)$	block power capacity for each stack technology, size, & number of stacks (MW)
$blockCost(k,l,m)$	investment cost for stack types for each stack technology, size, & number of stacks, & includes block level balance of plant (Mill. €)
C_0	base cost for a reference stack
C_{comp}	module cost of hydrogen/oxygen compressors
C_{cool}	bare module cost of inter coolers
C_{heat}	module cost of heaters
$C_{inv,curr}$	current balance of plant component of interest's investment cost
C_{pump}	bare module cost of pumps
C_{sep}	module cost of the hydrogen/oxygen separators
C_{stack}	investment costs of the electrolyzer stacks
$CapConv$	capital investment converter (Mill. €)
$CapEx$	capital expense of the system annualized over time (Mill. €)
$CapEx_{block}$	capital cost of an electrolyzer block, in the block optimization
cc_{cool}	commodity costs of cooling
cc_{elec}	commodity costs of electricity
cc_{heat}	commodity costs of heating
$CEPCI$	chemical engineering plant cost index
e	electricity tiers [wind, power purchase agreement, grid]
$EC(t)$	electricity consumption in any given time period (MW)
$ECE(t,e)$	electricity consumed in any tier in any given time period (MW)
$EP(t,e)$	electricity price at any time in any price tier (k€ MWh^{-1})
F	Faraday's constant
f	iteratively varied scalar used to optimize the system
F_p	cost factor for pressurized designs
G_{conv}	convectional heat losses
G_{cool}	required cooling demand of the block
G_{heat}	required heat demand of the block
h_{conv}	convective heat transfer coefficient
$HProd(j,k,l,m,t)$	hydrogen production rate in any time period of a specific block number, technology, size & number of stacks (kg s^{-1})
$HProdSys(t)$	total hydrogen production in any given time period (kg)
i	current density
j	block numbers
k	electrolyzer technologies [PEM_LP, PEM_HP, AWE_LP, AWE_HP]
k_1, k_2, k_3	cost fitting parameters
l	stack sizes [small, med, large]
$LCOH$	Levelized Cost of Hydrogen (€ kg^{-1})
$load_{min}$	minimal load of blocks (fraction)
M	cost scaling exponent
m	number of stacks per block [small, med, large]
n	lifetime of plant in years (years)

$O(j,k,l,m,t)$	binary variable for the activity (on / off) of a specific block number, technology, size & number of stacks combination
$OpEx(t)$	operating expenses of each time period (k €)
$OpEx_{block}$	operational costs of an electrolyzer block, in the block optimization
$OpMainRep$	annual cost of operations, maintenance, and stack replacement
p	stack pressure
P_{elec}	total block electrical power
p_{H2O}	water pressure
$Power(j,k,l,m,t)$	power loading level for a specific block number, technology, size & number of stacks in any given time (MW)
$powerBoP(j,k,l,m,t)$	power consumption of the balance of plant for a specific block number, technology, size & number of stacks in any given time (MW)
Q_{H_2}	total amount of hydrogen produced in a year (Mill. kg)
R	universal gas constant
r	discount rate
$rampDown(k,l,m)$	maximum ramp rate down as a fraction for each stack technology, size, & number of stacks (% hr^{-1})
$rampRateDown(k,l,m)$	rate at which electrolyzers can ramp down (MW)
$rampRateUp(k,l,m)$	rate at which electrolyzers can ramp up (MW)
$rampUp(k,l,m)$	maximum ramp rate up as a fraction for each stack technology, size, & number of stacks (% hr^{-1})
$SBoPE_{fix}(k,l,m)$	specific BoP electricity consumption offset / axis intercept for each stack technology, size, & number of stacks (MW)
$SBoPE_{var}(k,l,m)$	specific BoP electricity consumption for each stack technology, size, & number of stacks (MW per MW stack)
$SHP_{fix}(k,l,m)$	specific hydrogen production offset for each stack technology, size, & number of stacks (kg s^{-1})
$SHP_{var}(k,l,m)$	specific hydrogen production for each stack technology, size, & number of stacks (kg s^{-1} per MW)
$sysCap$	Overall system capacity (MW)
T	stack temperature
t	time periods
T_{amb}	ambient temperature
t_{mul}	length of time step in hours (hours)
$TotCost$	total cost to operate per year (Mill. €)
Δt	length of time steps in s (s)
U_{rev}	reversible stack voltage
$U_{rev,0}$	reversible stack voltage at standard conditions
U_{TN}	thermoneutral voltage
V	component capacity
$Y(j,k,l,m)$	binary variable for the existence of a block number, technology, size & number of stacks combination
ε	tolerance level for the optimization
ξ_{conv}	converter efficiency
τ	number of full load hours

List of Abbreviations

CO_2 – Carbon Dioxide
D&O – Design and operation
GHG – Greenhouse Gas Emissions
H_2 – Hydrogen
O_2 – Oxygen
LCOH – Levelized Cost of Hydrogen
AWE – Alkaline Water Electrolysis
PEMEC – Polymer Electrolyte Membrane Electrolysis
SOEC – Solid Oxide Electrolysis
BOP – Balance of Plant
LMTD – Log-Mean-Temperature-Difference
CEPCI – Chemical Engineering Plant Cost Index
MILP – Mixed Integer Linear Program
FLH – Full Load Hours
LP – Low Pressure
HP – High Pressure

1.0 Introduction

Over the coming years, the world's population will continue to grow, and more people will achieve higher standards of living, increasing the energy and commodity demands worldwide. Climate change is a serious concern, and these increased demands will only put further strain on global supply chains. The European Union has committed to reduce greenhouse gas emissions by 80-95%, while the United Kingdom has committed to total net zero greenhouse gas emissions [1,2]. New, low carbon technologies must be investigated and developed to achieve these ambitious targets. As a part of these greenhouse gas reduction efforts, industrial decarbonization must be considered, particularly with respect to feedstocks. Hydrogen is an important industrial feedstock and energy carrier which can be decarbonized through renewable energy.

Starting in the 20th century, hydrogen has become an integral part of the fuel industry for petroleum refining [3]. It is also heavily used in ammonia production, metal refining, and food processing. Since 1975, the annual demand for pure hydrogen has more than tripled to 70 Mt in 2018 [4]. Currently, hydrogen is primarily produced from steam methane reformation of natural gas, accounting for around three-quarters of annual pure hydrogen production. The balance of the hydrogen is created in the production of syngas from coal gasification (23% of hydrogen produced annually), and from water electrolysis (2% of hydrogen) [3]. This means that approximately 98% of pure hydrogen produced annually comes from fossil fuel sources, meaning there is still a heavy carbon burden associated with the production of hydrogen, around 830 million tons of CO_2 per year [3].

Hydrogen has the potential to fulfil other important roles in the future as well, for example as an alternative fuel as pure hydrogen, synthetic methane, ammonia or methanol [3]. It could also serve as an energy storage medium, as it can be stored in its pure form for later use [5–7]. The hydrogen can be used in fuel cells to convert the stored energy to electricity, or as a chemical feedstock and reductant. The process of generating gas as an energy storage medium from electricity is called Power-to-Gas. If hydrogen were generated through water electrolysis using renewable electricity, this would provide a potential green source for hydrogen, thus decarbonizing these industrial processes.

Electrolysis has been a source of interest for a long time, but has been gaining popularity in recent years as a green source for hydrogen [8–10]. There are three main technologies employed in electrolysis: alkaline water electrolysis (AWE), polymer electrolyte membrane electrolysis (PEMEC), and solid oxide electrolysis (SOEC). Of these three, AWE is the oldest and most commercially developed [11]. In AWE, the anode and cathode bipolar plates are separated by a membrane which is only permeable to hydroxide ions, but not to protons, H^+, which separates the gas evolution & ions. AWE electrolyzers are supplied with liquid alkaline electrolytes, such as sodium hydroxide or potassium hydroxide in an aqueous solution, rather than pure water or acid, improving performance through increased ion conductivity and reducing corrosion losses [4]. This allows for long stack lifetimes, well into the tens of thousands of hours [12]. Further, they do not use expensive platinum-group metals, reducing the cost of these designs [4,13]. Lee et al demonstrated the continued importance of AWE for hydrogen production now and into the future, due to improvements in the technology [14].

Polymer electrolyte membrane electrolyzers are a newer technology, which are still being developed, but are available commercially in smaller units than in AWE. This type of electrolysis also requires anode and cathode bipolar plates to be separated by a membrane,

however, in this scenario, the membrane is only permeable to hydrogen ions, or protons, but not to hydroxide ions. This again separates the ions and half reactions to each side of the membrane. PEM electrolyzers are supplied with pure water, rather than a basic solution, meaning the inside of a PEMEC is very acidic due to the concentration of hydrogen ions. This necessitates the use of expensive platinum-group metals to prevent corrosion [15]. These designs benefit from the ability to more easily handle partial load during operation and that they can handle much higher current densities than alkaline water electrolyzers, both of which increase their flexibility [16]; they also represent a more intensified technology.

Solid oxide electrolyzers are still in the research stage and have not been extensively commercialized yet. These electrolyzers have the potential for higher efficiencies than either PEMEC or AWE units due to significantly elevated temperatures [17]. However, since these designs have not been commercialized, they are not examined in this work.

Historically, electrolyzers have used electricity from a steady power source, such as hydroelectric power from a dam [4]. The low cost of hydroelectric power, combined with the advantage of a steady power source, benefitted the business case. More recently, there has been some research recently into connecting electrolyzers to intermittent power supplies, usually wind.

There have been several studies on the operation and use of electrolyzers under different power supply conditions. One study by Jorgensen and Ropenus studied the prices of hydrogen from an electrolyzer connected to a grid with high wind penetration, and found that electrolyzers can be used to effectively balance the grid, and to uptake excess wind production, but that the hydrogen produced is more expensive than established targets [18]. Troncoso and Newborough explored using electrolyzers to mitigate wind curtailment by having a readily available load to uptake excess wind power. They found the cost of hydrogen from these systems to be slightly more expensive, in the range of $20-30 per kg, but that it increased the viability of wind power plants [9]. Zhang and Wan also studied the use of electrolyzers to uptake excess electricity from wind farms, rather than using wind curtailment, and they found that the hydrogen produced in this way would be cheaper than hydrogen produced by pulling electricity from the grid [19]. Green, Hu, and Vasilakos studied how introducing large electrolyzers would affect the electrical grid and capacity mix. They found that while the hydrogen produced from these electrolyzers would be more expensive than the hydrogen produced by natural gas, it would encourage the integration of wind power into the grid [20]. Bennoua et al. further described how electrolyzers could act as a balancing mechanism for the electrical grid [21]. Loisel et al. performed a study on the economics of combining an offshore wind farm with a hydrogen production facility, and found that the only way to make such a system economically viable was to limit the number of potential end uses for the hydrogen & power to only a couple energy products, rather than trying to provide broad usability across a range of scenarios [5].

Other studies have integrated a way of using hydrogen, such as storage, fuel cells, or hydrogen fueling stations, into the system that is being examined to understand how electrolyzer operational strategies affect the end use. Grueger et al. demonstrated how an electrolyzer and fuel cell combination could be used to reduce forecasting errors in the power produced by a 100 MW wind farm through electrolysis production of hydrogen during positive forecast errors, and fuel cell consumption of hydrogen during negative forecast errors [22]. Chang et al. examined the possibility of integrating an electrolyzer / fuel cell system into large-scale wind farm in Taiwan in 2025, and found that this could increase the available energy by up to 7% [23]. Menanteau et al., who examined the impact of various electrical supply and hydrogen

demand scenarios for a wind-electrolyzer combination found that hydrogen storage made hydrogen very expensive, but that the size of necessary storage could be reduced by connecting the system to the grid to supplement electricity when needed [24]. Rahil et al. examined the impact of operational strategy for a small-scale electrolyzer on the cost of hydrogen produced, and found that the cheapest hydrogen was produced when the electrolyzer used off-peak electricity, rather than continuously operating [10]. Dagdougui et al. examined a supply chain where local hydrogen refueling stations are supplied by a central electrolyzer with storage which is powered by a mix of wind and solar, developing a mathematical programming model which could satisfy the demand at all refueling stations at all times [25]. Kim et al examined connecting an electrolyzer to a blast furnace in the steel sector, finding that it would reduce the total carbon dioxide released in steelmaking [26].

Another important area of research investigates the economic performance of electrolyzer systems under a range of conditions. Lee et al performed a techno-economic analysis of major hydrogen generation technologies, including electrolysis, at several scales for use in Korea. They found that scale is very important in the final cost of the hydrogen, for which technology may be the best choice [27]. Yates et al performed a techno-economic analysis on combining photovoltaics with electrolyzers for off grid applications, finding the effectiveness is dependent on how much energy the photovoltaic cell produces [28]. Gallardo et al examined the potential for hydrogen production from solar power in the Atacama desert, and found that it can be extremely cost competitive with other hydrogen production technologies [29]. Sadeghi et al investigated several methods of producing hydrogen, such as steam methane reforming, coal gasification, photovoltaic electrolysis, and solar thermal electrolysis, demonstrating that while photovoltaic electrolysis is more expensive than classical methods of producing hydrogen, it is also significantly more environmentally friendly [30].

Many of these previous works focus on the operation of an electrolyzer system, rather than the design. However, an important knowledge gap that these previous works largely do not address is the design and operation interdependency. In larger systems, the design and operation of the system is a particularly conjoined problem – the way the system is designed will limit the ways it can operationally respond to changing loads or demands, and conversely, how the system needs to respond to changing loads or demands will affect the necessary design. This paper is novel by adding design as a decision variable which can be optimized to the more traditional operational optimizations.

This paper seeks to fill this knowledge gap by providing a framework by which the design and operational strategy of a large-scale wind powered hydrogen electrolyzer may be optimized. In this work, the goal is to minimize the levelized cost of hydrogen (LCOH), to make the hydrogen produced as cheap as possible. While the focus of this work is economic, the framework could also be used to optimize the design and operation for any other objective, such as an environmental objective, with the appropriate modification to the objective function. Also, the large size means there will be multiple stacks in the system, presenting interesting opportunities for more complex responses to changing operational load. These considerations imply the necessity for and novelty of a framework for the systematic design and operational strategy of large-scale hydrogen electrolyzers.

Section 2.1 of this paper defines the problem statement, then in section 2.2 presents the mathematical formulations of the problem of optimal design and operation at two levels, and finally in section 2.3 describes the case study of interest. Section 3 discusses the results of

applying the framework to the case study. Section 4 concludes the work by reviewing the framework and the results.

2.0 Materials & Methods

2.1 Problem Statement

In this work, a framework is developed for the optimal design and operational strategy for a large-scale water electrolyzer powered by wind. Large-scale hydrogen production is a necessary precursor for many hydrogen-powered technologies to be viable [31], and would provide opportunities for industrial decarbonization in many sectors. The framework will determine the appropriate number of electrolyzer stacks & their associated size, how those stacks should be grouped, what size the balance of plant components must be to accommodate those stacks, and how to operate the system to respond to power availability and price.

The goal of the framework is to minimize the LCOH, so that hydrogen produced by the system is as cheap as possible. The framework is flexible and can be used to determine the optimal design and operation of an electrolyzer system given any input scenario, including alternative power profiles & power costs, alternative system & stack sizing, alternative technology choices, or even use an alternative objective function rather than LCOH.

This design problem necessitates multiscale modelling to accurately capture the behavior of the system and its constituent components. This structure is addressed through the use of two levels of optimization. The first level uses a general process modelling system called gPROMS to optimize the design of an individual electrolyzer modular block, composed of an electrolyzer stack(s) and some associated balance of plant components. Thus, the design of an electrolyzer block for achieving a given power level is obtained, and then that design is simulated in gPROMS to determine the partial load behavior. The second level uses the output of the gPROMS optimization in a system level optimization constructed in the mathematical modelling system called GAMS, to determine the optimal number, type, and combination of electrolyzer blocks to minimize the LCOH for a given range of hydrogen production rates.

The framework takes the following as inputs:
- Time profile of available power from all sources
- Time profile of associated cost of power
- Hydrogen & oxygen delivery pressure
- Electrolyzer system power capacity
- Power electronics efficiency
- Maximum current density for each electrolyzer technology
- Faradaic efficiency
- Operating temperature
- Electrolyzer ramping rates
- Minimum load calculation
- Lifetime of plant
- Discount rate
- System cost (outside of stack & some balance of plant components)
- Baseline stack cost estimates and associated stack sizes

The framework produces the following output:
- Levelized cost of hydrogen
- Optimal stack size, technology, number of stacks, and operating pressure
- Time series of hydrogen produced over the production horizon

- Capital cost of the optimal design
- Operating costs of the optimal design
- Operational strategy for the power profile provided

2.2 Mathematical Formulation

2.2.1 Block Design

Electrolyzer blocks represent repeating, modular units in the electrolyzer system. The central elements of an electrolyzer block are the electrolyzer stacks and the relevant block-level balance of plant (BOP) components. BOP components are included in the block flowsheet if they either have an influence on the block design, e.g., preheating, or must be represented by multiple units in the electrolyzer system such as compressors. The BOP components included are a water preheater, gas separators, gas compressors and a feed water pump if electrolysis takes place at pressurized conditions. If multiple compression stages are required, the process flowsheet contains intercoolers.

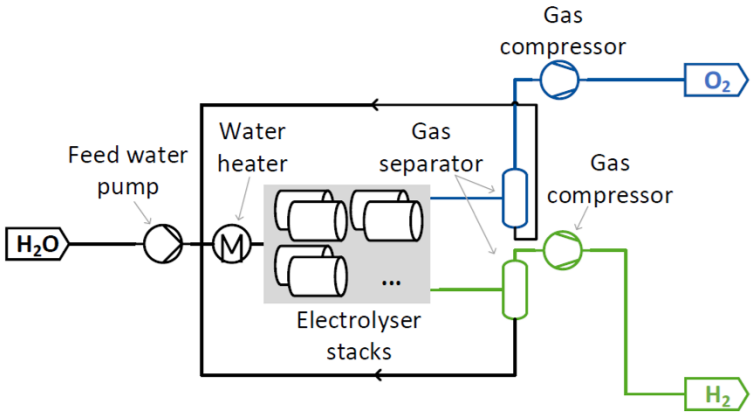

Figure 1: The flowsheet of a generic electrolyzer block. Depending on the particular block in question, some details may change, such as number of compressors, or the presence of a feed water pump.

Each combination of electrolyzer block is implemented in the electrolyzer system model, examining electrolyzer technology (AWE, PEMEC), electrolyzer pressure (ambient, pressurized), stack power capacity (1, 5, 10 MW stack sizes), and stack number (1, 5, 10 stacks per block), giving 36 different electrolyzer block designs. Electrolyzer technology and pressure variants are implemented to investigate cost and operational aspects. Ambient pressure systems require expensive hydrogen compression, whereas the investment costs for pressurized electrolyzer stacks are higher. The electrolyzer pressure is introduced as a discrete design decision in the system model since electrolyzer cost functions dependent on the electrolyzer pressure are not available. Stack numbers and power capacities are implemented to investigate economy of scale effects of electrolyzer stacks and BOP components.

To model the variations on block level, all components are represented in the respective flowsheets. Capital expenditures of an electrolyzer block, $CapEx_{block}$ are defined as a modification of cost equations from Turton et al [32] and Bejan & Moran [33]:

$$CapEx_{block} = C_{stack} + 3.7 * \left(C_{heat} + C_{comp} + C_{sep} + C_{pump} + C_{cool}\right) \qquad \text{Eq. 1}$$

where C_{stack} is the investment costs of the electrolyzer stacks, C_{heat} is the module cost of the heater, C_{comp} is the module cost of the hydrogen/oxygen compressors and C_{sep} is the module cost of the hydrogen/oxygen separators. C_{pump} is the bare module costs of the pump and C_{cool} is the bare module costs of the inter coolers, either of which are only included if the flowsheet

contains these components. The cost factor of 3.7, which incorporates additional costs such as installation or planning, is taken from the literature [33,34].

When operating an electrolysis block, mainly four commodities are required: water, electricity, cooling and heating. In this work, it is assumed that water costs are based on a constant annual fee. Therefore, the operational costs of an electrolyzer block are described as $OpEx_{block}$

$$OpEx_{block} = \tau * \left(cc_{elec} * P_{elec} + cc_{heat} * \dot{Q}_{heat} + cc_{cool} * \dot{Q}_{cool}\right) \quad \text{Eq. 2}$$

$$P_{elec} = P_{elec,stack} + P_{elec,BoP} \quad \text{Eq. 3}$$

$$\dot{G}_{cool} = \dot{G}_{cool,stack} + \dot{G}_{cool,BoP} \quad \text{Eq. 4}$$

$$\dot{G}_{heat} = \dot{G}_{heat,stack} + \dot{G}_{heat,BoP} \quad \text{Eq. 5}$$

where cc_{elec}, cc_{heat} and cc_{cool} are the specific commodity costs of electricity, heating, and cooling. τ is the full load hours, P_{elec} the total block electrical power, G_{heat} the required heating demand and G_{cool} the required cooling demand of the block. The subscripts stack and BoP indicate the properties caused by stacks and the balance of plant of the block, respectively. The required cooling G_{cool} / heating G_{heat} demand is equal to the cooling/heating demands of the electrolyzer stacks and of the BOP.

The electrolyzer model is essential for the block design and for determining the partial load behavior of electrolyzer blocks. To model the reversible stack voltage U_{rev}, we use a simplification of the Nernst equation which is valid if product gases are considered wet and the pressures at cathode and anode are equal [35]:

$$U_{rev} = U_{rev,0} + \frac{RT}{2F} \ln\left(\frac{1.5 * \left(p - p_{H_2O}\right)}{p_{H_2O}}\right) \quad \text{Eq. 6}$$

Where $U_{rev,0}$ is the reversible stack potential at standard conditions, R is the universal gas constant, F is Faraday's constant, T & p are stack temperature & pressure, and p_{H2O} is the water pressure.

Different approaches are used for AWE and PEMEC electrolyzers to calculate stack voltage. For AWE stacks the polarization curve uses a form commonly found in the literature but the parameters are specific to experiments conducted by partner members of the Hydrohub Gigawatt Scale Electrolyzer project [36,37]:

$$U_{cell} = U_{rev} + C_1 + C_2 * \log\left(\frac{i}{C_3}\right) + C_4 * i \quad \text{Eq. 7}$$

where i is the current density. This modelling approach does not reflect temperature dependency of the voltage, so the model was fitted for a fixed temperature of electrolysis of 90°C.

The PEMEC overvoltages are modelled as proposed by Garcia-Valverde et al. [38,39]. This form is similar to the AWE modelling. However, many of the parameters are temperature

dependent, the parameter values are taken from the references rather than partner experiments, and finally, there is no addition of an extra constant to the reversible voltage.

$$U_{cell} = U_{rev} + \frac{RT}{nF} * \ln\frac{i}{i_0(T)} + R_I(T) * i \quad \text{Eq. 8}$$

The product gas streams are assumed to be fully saturated with water coming out of the stack. In this work, gas crossover in either direction is not considered.

Finally, a thermal model is required to estimate the cooling/heating demand for the electrolyzer stacks. In this work, a simplified thermal model for a quasi-static lumped capacitance is applied. In this model, it is assumed that inlet and outlet temperature are equal and, therefore, the following simplified energy balance is derived for the cooling demand of the stack [35]:

$$\dot{Q}_{cool,stack} = (U_{stack} - U_{TN}) * i - \dot{Q}_{conv} \quad \text{Eq. 9}$$

Where U_{TN} is the thermoneutral voltage. The convectional heat losses Q_{conv} are generally small compared to the cooling demand but a simple model for estimation of convectional heat losses is considered [35]:

$$\dot{Q}_{conv} = A_{surf} * h_{conv} * (T - T_{amb}) \quad \text{Eq. 10}$$

where A_{surf} is the estimated surface area of the electrolyzer stack, h_{conv} the convective heat transfer coefficient, T the electrolyzer temperature and T_{amb} the ambient temperature.

In addition to the technical modelling of the electrolyzer stacks, economic modelling is required to enable techno-economic optimization. Typically, investment cost functions for electrolyzers are available as a function of power capacity. However, given that current density is a design choice, and that stack area is the main cost driver due to material usage, the stack investment cost, C_{stack}, should be a function of stack area, A_{stack}. This cost function follows the form of some cost functions defined in Turton et al [32]:

$$C_{stack} = F_P * C_0 * \left(\frac{A_{stack}}{A_0}\right)^M \quad \text{Eq. 11}$$

where F_p is a pressure factor which represents that pressurized stacks are more expensive than ambient pressure stacks, C_0 is the base cost for a reference stack, A_{stack} is the electrolyzer stack area, A_0 the base stack area for a reference stack and M a cost scaling exponent.

Pumps and compressors are modelled using gPROMS built-in technical models. The feed water pump is modelled as a centrifugal pump with an isentropic efficiency of 0.8 and a mechanical efficiency of 0.9 [40]. The compressors are modelled as centrifugal compressors, also with an isentropic efficiency of 0.8 and a mechanical efficiency of 0.9 [40,41]. The maximum compression ratio for compressors before intercoolers are introduced to prevent overheating is 3 for H_2, and 4 for O_2. The intercoolers, the preheater and the gas separators also use models implemented in the software as simple plate heat exchangers. The gas separators use an outlet temperature of 25°C for the cooling demand calculations. The heat exchangers are sized using the log mean temperature difference method (LMTD) with an assumed temperature difference

of 15°C [42]. Cost correlations for component sizing follow the form and fitting values proposed by Turton et al [32]:

$$C_{inv,curr} = \left(\frac{CEPCI_{curr}}{CEPCI_{ref}}\right) * 10^{[k_1 + k_2 * \log V + k_3 * \log(V)^2]} \quad \text{Eq. 12}$$

Where $C_{inv,curr}$ is the current component of interest's investment cost, $CEPCI$ is the chemical engineering plant cost index, used here to scale prices to the model year, which is 2017, k_1, k_2, and k_3 are fitting parameters, and V is the capacity.

In addition to the design, the partial load behavior of the block is determined in gPROMS. This is necessary for understanding how the hydrogen production rate and BOP operation energy usage change under different loading scenarios when the system is operating at partial load. The data sets for both the hydrogen production rate, and BOP energy usage are fitted to linear correlations for use in the system optimization, which is a linear optimization problem. Once linearized, the resulting y-axis intercept and the slope of the linearizations are transferred to the system optimization.

2.2.2 System-Level Formulation

The final system design and associated operational performance is calculated using a Mixed Integer Linear Program (MILP). The program takes as inputs the outputs from the gPROMS block models (block size, capital cost, partial load behavior of hydrogen production, partial load behavior of the balance of plant energy usage), information about the availability & cost of electricity, and information about the ramping rates of electrolyzer designs. It uses this information to calculate the optimal number, capacity, technology type for blocks to satisfy the design constraints, and calculates the optimal dynamic load for all blocks over all time periods in the optimization.

The objective function to be minimized is the $LCOH$, which is the total annual cost of the system over the year, $TotCost$, divided by the total quantity of hydrogen produced, Q_{H_2} [43]:

$$LCOH = \frac{TotCost}{Q_{H_2}} \quad \text{Eq. 13}$$

This objective function (minimization of LCOH) is nonlinear, however, so it is instead optimized iteratively using the Dinkelbach algorithm, with a scalar f, originally initialized to an arbitrarily large value [44,45]:

$$min\left[TotCost - f * Q_{H_2}\right] \quad \text{Eq. 14}$$

The Dinkelbach algorithm is a method of linearizing certain nonlinear families of objective functions when the rest of the problem is also linear. By using this method to linearize the objective function, it ensures that a globally optimal solution will be converged upon. Optimized variables for the values are denoted as $TotCost^*$ and ${Q_{H_2}}^*$. From here, an evaluation must be made to determine if the solution to the min (LCOH) problem has been obtained, by comparing the optimized values for the variables to an error tolerance value, ε, [44,45]

$$\left|TotCost^* - f * {Q_{H_2}}^*\right| \leq \varepsilon \quad \text{Eq. 15}$$

If the left-hand-side is less than the tolerance value, the solution to the LCOH optimization problem has been determined. The value of ε is dependent on the problem and does not have a standard value. Otherwise, the value f must be updated as below, and the minimization must be re-run, [44,45].

$$f = \frac{TotCost^*}{Q_{H_2}^*} \quad \text{Eq. 16}$$

The total cost over the planning horizon is defined as the sum of all operating, *OpEx(t)*, over all time periods, *t*, plus the capital expenditure, *CapEx*, of purchasing the necessary units multiplied by the annualization factor [26]:

$$TotCost = AF * CapEx + \sum_t OpEx(t) \quad \text{Eq. 17}$$

The formula for the annualization factor is dependent on the annual discount rate, *r*, and the project lifetime in years, *n*. Based on conversations with project partners the discount rate was set to be 8%, the project lifetime was assumed to be 15 years, and all costs / profits are normalized to the first year of the project [46].

$$AF = \frac{r * (1+r)^n}{((1+r)^n - 1)} \quad \text{Eq. 18}$$

The capital cost is the total sum of the cost of each block, *j*, of technology, *k*, size, *l*, and number of stacks, *m*, *blockCost(k,l,m)*, plus an estimate of the capital cost of the balance of plant that is not included in the gPROMS balance of plant costing estimates, *CapEst*. The binary existence variable, *Y(j,k,l,m)*, ensures that only blocks which have been built in the optimization are counted.

$$CapEx = \sum_{j,k,l,m} Y(j,k,l,m) * blockCost(k,l,m) + CapEst \quad \text{Eq. 19}$$

The operational expenses are the cost of electricity in each price tier over the time horizon, *EP(t,e)*, multiplied by the amount of electricity used, *ECE(t,e)*, all multiplied by the length of a time period, and summed for each price tier for each period of the planning horizon. Electricity tiers are based on the source of the electricity, for example from the wind plant, or from potential power purchase agreements, plus the annual cost of operations, maintenance, and stack replacement, *OpMainRep*.

$$OpEx(t) = \sum_e ECE(t,e) * EP(t,e) * t_{mul} + OpMainRep \quad \text{Eq. 20}$$

Note that this variable, OpEx(t), differs from the $OpEx_{block}$ variable introduced in the previous section, as OpEx(t) is the operational expenses of the entire optimized system, with varying load distribution across multiple potentially different blocks, rather than the operational expenses of a single block. The existence variable, *Y(j,k,l,m)*, is 1 when a particular block number, size, and technology type combination is selected to be built, and 0 otherwise.

$$Y(j,k,l,m) = \begin{cases} 1 & if\ a\ block\ with\ particular\ combination\ j,k,l\ exists \\ 0 & otherwise \end{cases} \quad \text{Eq. 21}$$

The operation variable, *O(j,k,l,m,t)*, is 1 when a particular block number, size, and technology type combination is turned on in time period t producing hydrogen, and 0 otherwise.

$$O(j,k,l,m,t) = \begin{cases} 1 & if\ a\ block\ with\ particular\ combination\ j,k,l\ is\ on \\ 0 & otherwise \end{cases} \quad \text{Eq. 22}$$

To ensure the optimization only turns on blocks that are built, the operation variable must be set to be less than or equal to the existence variable.

$$O(j,k,l,m,t) \leq Y(j,k,l,m) \quad \text{Eq. 23}$$

To prevent the optimization from searching through multiple equivalent configurations, a degeneracy condition is imposed upon the binary variable *Y(j,k,l,m)* indicating the existence of a particular combination of block number, technology type, and size. The degeneracy condition ensures that the block numbers start with 1 and count sequentially up.

$$Y(j,k,l,m) \leq Y(j-1,k,l,m) \qquad \forall\ j > 1 \quad \text{Eq. 24}$$

To prevent further degeneracy regarding the order of existing blocks, another degeneracy condition is implemented to ensure that the largest blocks are always listed first, using the size of available blocks *blockCap(k,l,m)*.

$$Y(j,k,l,m) * blockCap(k,l,m) \leq Y(j-1,k,l,m) * blockCap(k,l,m) \quad \forall\ j > 1 \quad \text{Eq. 25}$$

The power used by a specific block's balance of plant in any time period, *powerBoP(j,k,l,m,t)*, is given by the corresponding fixed energy demand, $SBoPE_{fix}(k,l,m)$, multiplied by the operational variable (to ensure this is not counted when the block is off), plus the specific rate of energy usage, *SBoPE(k,l,m)*, multiplied by the stack power.

$$powerBoP(j,k,l,m,t) = SBoPE_{fix}(k,l,m) * O(j,k,l,m,t) + SBoPE(k,l,m) * Power(j,k,l,m,t) \quad \text{Eq. 26}$$

The electricity consumed by the system, *EC(t)*, is the sum of stack power and block level balance of plant power, summed over all blocks, divided by the efficiency of the power conversion system, ξ_{conv}.

$$EC(t) = \sum_{j,k,l,m} \frac{Power(j,k,l,m,t) + powerBoP(j,k,l,m,t)}{\xi_{conv}} \quad \text{Eq. 27}$$

The sum of electricity used in each tier in each time period, *ECE(t,e)*, must be equal to the total amount of electricity used by the system, *EC(t)*.

$$EC(t) = \sum_{e} ECE(t,e) \quad \text{Eq. 28}$$

The amount of electricity used in each tier must be less than the amount of electricity available in each tier, *AE(t,e)*.

$$ECE(t) \leq AE(t,e) \quad \text{Eq. 29}$$

The hydrogen produced by a specific block in any time period, *HProd(j,k,l,m,t)*, is given by the corresponding hydrogen production curve's axis intercept, $SHP_{fix}(k,l,m)$, multiplied by the operational variable (to ensure this is not counted when the block is off), plus the specific hydrogen rate of production, *SHP(k,l,m)*, multiplied by the stack power.

$$HProd(j,k,l,m,t) = SHP_{fix}(k,l,m) * O(j,k,l,m,t) + SHP(k,l,m) * Power(j,k,l,m,t) \quad \text{Eq. 30}$$

The hydrogen production of the entire system in any time period, *HProdSys(t)*, is the sum of the hydrogen production rate for all blocks multiplied by the number of seconds per time step, Δt.

$$HProdSys(t) = \sum_{j,k,l,m} HProd(j,k,l,m,t) * \Delta t \quad \text{Eq. 31}$$

The amount of hydrogen produced during the planning horizon of the system, Q_{H_2}, is the sum of system hydrogen production in all time steps, converted to tons produced.

$$Q_{H_2} = \sum_{t} \frac{HProdSys(t)}{10^3} \quad \text{Eq. 32}$$

The power of a block is also limited to be less than its maximum design power, ensuring the power used by the block does not exceed what the block is designed for.

$$Power(j,k,l,m,t) \leq blockCap(k,l,m) * O(j,k,l,m,t) \quad \text{Eq. 33}$$

The power of the block is bounded to be greater than the minimum load of the block, if the block is active, otherwise it is 0.

$$Power(j,k,l,m,t) \geq load_{min} * blockCap(k,l,m) * O(j,k,l,m,t) \quad \text{Eq. 34}$$

The amount by which electrolyzer block can change operation from time step to time step is defined by the ramping rates *rampRateDown(j,k,l,m)* & *rampRateUp(j,k,l,m)*. These rates are calculated from a block specific fractional ramping rate, *rampDown(k,l,m)* & *rampUp(k,l,m)*, multiplied by the block's capacity and the timestep length, t_{mul}.

$$rampRateDown(j,k,l,m) = rampDown(k,l,m) * blockCap(k,l,m) * t_{mul} \quad \text{Eq. 35a}$$
$$rampRateUp(j,k,l,m) = rampUp(k,l,m) * blockCap(k,l,m) * t_{mul} \quad \text{Eq. 35b}$$

The actual change in power consumed by the blocks from one timestep to the next is bounded by the above ramping rates.

$$Power(j,k,l,m,t) \geq Power(j,k,l,m,t-1) - rampRateDown(j,k,l,m) \quad \forall\, t > 1 \quad \text{Eq. 36a}$$
$$Power(j,k,l,m,t) \leq Power(j,k,l,m,t-1) + rampRateUp(j,k,l,m) \quad \forall\, t > 1 \quad \text{Eq. 36b}$$

The total power capacity of the system, which is the sum of all existing block capacities, must be equal the total system capacity specified (which in this case is 1 GW), *sysCap*.

$$sysCap = \sum_{j,k,l} Y(j,k,l,m) * blockCap(j,k,l,m) \quad \text{Eq. 37}$$

2.3 Case Study

The performance of the framework was explored using the case study of an electrolyzer powered by a 1-gigawatt scale offshore wind farm in the Netherlands, based on the ISPT HydroHub project [47]. The goal was to minimize the levelized cost of hydrogen produced by the plant through optimal design and operation decisions, and to understand the viability of large-scale electrolysis as an alternative to conventionally produced hydrogen. The system was optimized over a quarter-year, to limit the computation time. The system is assumed to have a 15-year lifespan, with a discount rate of 8% on the capital cost of the system. The minimum load is 15% of the maximum load for the entire plant.

To better understand how the framework responds to changes in inputs, three different electricity profiles were used as a starting point. All power profiles provide equivalent total energy, so they are comparable. The first profile provides the system with a constant power supply equal to the average utilization of the wind profile, also known as equivalent full load hours (Eq. FLH). This is used as a reference. The second power profile is a wind power profile obtained from the renewablesninja website [48–50], with data points at every hour for a quarter year (Wind). The profile was obtained for a theoretical oceanic wind farm located off the coast of the Netherlands near Rotterdam. The final power profile is the same wind profile as profile two, Wind, but compressed in time by a factor of four, so the data points reflected a quarter-hour (Wind Qtr), where all relevant optimized quantities are multiplied by four to reflect the entire time horizon. These profiles provided the same energy with system full load hours of 3983 hours, but were different temporally, and used to elicit potential differences in design choices in the framework.

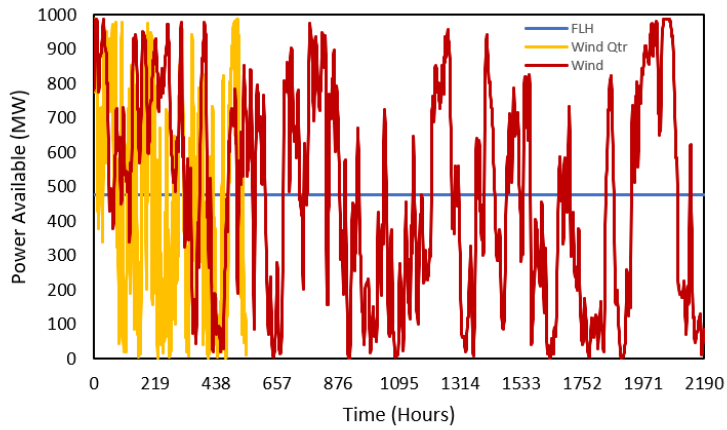

Figure 2: The power profiles used in this study

For this case study, the technology choices were limited to Alkaline Water Electrolysis (AWE), and Proton Exchange Membrane Electrolysis (PEMEC). Both technologies are mature enough that they could feasibly be commercially scaled up to supply a 1 GW plant. Other technologies, such as solid oxide electrolyzers, or anion exchange membrane electrolyzers are not sufficiently commercially advanced to be scaled up in such a manner [51].

Two choices for the operating pressure of the electrolyzer were selected – one at atmospheric conditions (LP), and one where the electrolyzer was operated at the delivery pressure of the hydrogen, 30 bar (HP). These were selected to understand the impact of the presence of compressors after electrolysis on the final performance of the system. Finally, both the stack size and the number of stacks in a block are variables. To reduce the search space, three stack sizes, and three numbers of stacks per block were selected as available options for the optimization. The stack sizes selected were 1 MW, 5 MW, and 10 MW stacks based on industrially sized systems [36,52], and the options for the number of stacks per block are 1 stack, 5 stacks, and 10 stacks.

The cost for the rest of the plant above the cost of the stacks and associated balance of plant components discussed previously, *CapEst*, is assumed to be 1000 M€. Further, annual maintenance, operation, and stack replacement costs, *OpMainRep*, are estimated to be 10% of the total block cost. These values come from discussion with experts in the field.

Table 1: Key parameters of the optimization and the values associated with them

Parameter Symbol	Description	Value	Reference
$\eta_{comp,is}$	Isentropic Compressor Efficiency	0.8	[40]
$\eta_{comp,mech}$	Mechanical Compressor Efficiency	0.9	[40]
$\eta_{pump,is}$	Isentropic Pump Efficiency	0.8	[40]
$\eta_{pump,mech}$	Mechanical Pump Efficiency	0.9	[40]
	Max Pressure Ratio H2	3	[53]
	Max Pressure Ratio O2	4	[53]
T_{cool}	Temperature of Cooling Water [°C]	25	
	Faradaic Efficiency	98%	[37]
T_{PEM}	Operating Temp PEM [°C]	80	[36]
T_{AWE}	Operating Temp AWE [°C]	90	[4]
$CEPCI_{curr}$	Chemical Engineering Plant Cost Index, Current Year (2017)	567.5	[54]
$CEPCI_{ref}$	Chemical Engineering Plant Cost Index, Reference Year (2001)	394	[32]
F_p	Cost scaling factor for pressurized electrolysis	1.2	[55]
M	Cost scaling exponent for area scaling	0.9	[55]
$A_{0,PEM}$	Base active area size for a reference PEM electrolyzer [m^2]	28	[56]
$A_{0,AWE}$	Base active area size for a reference AWE electrolyzer [m^2]	97	[4]
$C_{0,PEM}$	Base cost for a reference PEM electrolyzer [€ m^{-2}]	36000	[12]
$C_{0,AWE}$	Base cost for a reference AWE electrolyzer [€ m^{-2}]	8300	[12]
T_{amb}	Ambient temperature [°C]	25	
h_{conv}	Convective heat transfer coefficient [W m^{-2} K^{-1}]	4.3	[57]
U_{TN}	Thermoneutral voltage [V]	1.48	[57]
ξ_{conv}	Electrical Converter Efficiency	95%	[58]
$load_{min}$	Block Minimum Load Level	15%	[36]
r	Discount Factor	8%	[58]
n	Project Lifetime [years]	15	[58]
$rampRateUp$	Rate electrolyzer can increase the load (AWE, PEM) [% / hr]	50, 100	
$rampRateDown$	Rate electrolyzer can decrease the load (AWE, PEM) [% / hr]	75, 150	
EP	Cost of Wind (for all time periods) [€ MW^{-1}]	40	[59,60]

The system design was performed in gPROMS ProcessBuilder 1.5.0. The MILP was formulated in GAMS 25.0.3 and solved using CPLEX 12.8.0.0.

3.0 Results & Discussion

3.1 Block Design

The block design method was successfully able to optimize the design and cost for all the variations of block designs examined in the case study used to illustrate the framework developed here. Both the total cost of the entire block, and the cost per MW of the block can be found in Figure 2. The total cost for blocks goes up as both the individual stack size increases, and as the number of stacks per block increases. The designs with 10 MW stacks are the most expensive to build, costing millions of euros more per block than the smaller stacks. Blocks with ten stacks are also the most expensive to build, costing millions or even tens of millions of euros more to build than a single stack per block. The high-pressure designs are generally less expensive to build than an equivalent low-pressure design, despite needing higher quality designs and more material. This is due to savings on not needing large, expensive compressors, reducing the total capital cost. Further, AWE designs are cheaper than PEM designs, in all cases. This is because PEM is a newer technology, and because these designs use rare, expensive metals, raising the total cost. Together, this means that the cheapest design is a block with a single 1 MW stack that is high pressure and AWE, while the most expensive block is ten stacks of 10 MW each, which are low pressure and PEM. All of this is as expected, as these designs are the ones that require the most material and are the most complicated.

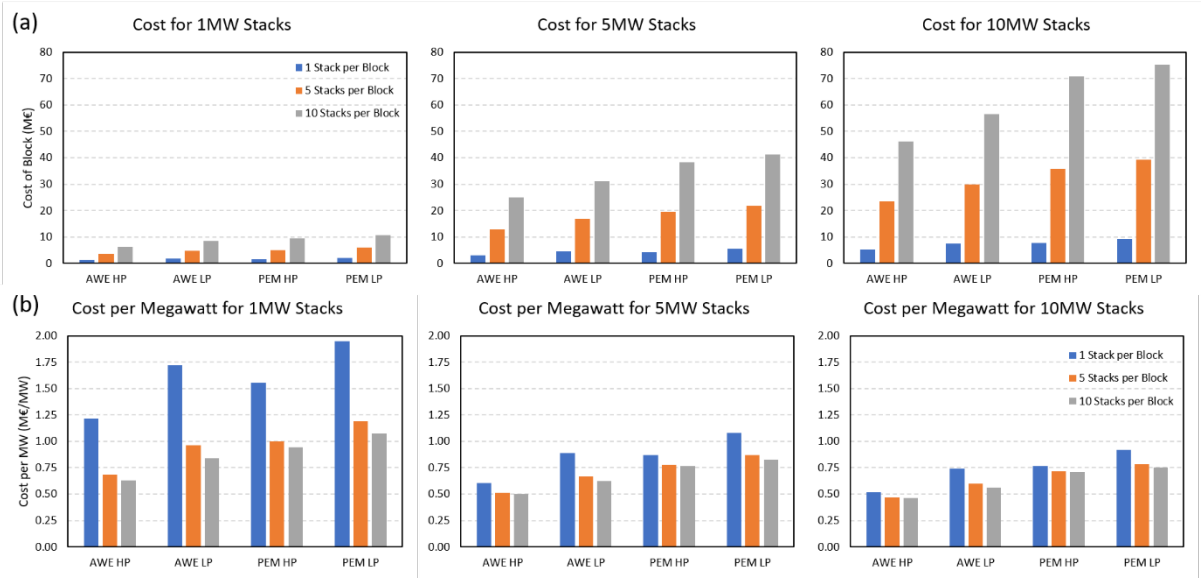

Figure 3: The cost for each electrolyzer block type in (a) M€ and (b) M€ per MW

When looking at the cost per MW of blocks, however, the results present a slightly different story. From this view, increasing stack size reduces the cost of blocks, such that the blocks which use the 10 MW stacks are the cheapest. Further, increasing the number of stacks also reduce the cost, where the designs with 10 stacks per block are the cheapest. This comes from economies of scale. Larger block sizes allow for larger balance of plant components. These tend to become relatively cheaper as size increases, reducing the per MW cost of the block. Both PEM and low-pressure designs tend to be more expensive per MW, for similar reasons as previously stated. This is similar to the total capital cost, as technology type and pressure do not impact the number of megawatts of stacks in a block.

As previously discussed, part of the function of the block level optimization and modelling is to determine the partial load behavior of blocks. Inevitably, blocks will not be able to operate at full load, and so understanding the energy consumption and hydrogen production rates at partial load is critical. The power consumed by stacks was compared against the hydrogen

production rate of the block or the balance of plant power usage. To keep the mathematical program as a linear problem, the partial load behavior was linearized. The linearized values of each block technology type are listed in Table 2.

Table 2: The specific hydrogen production rate of each technology (in kg s^{-1} (MW stack)$^{-1}$) and the specific balance of plant electricity usage (in MW (BoP) MW (Stack)$^{-1}$)

Technology Type	Specific H_2 Production Rate	Specific BoP Power Use
AWE HP	0.00508	0.0087
AWE LP	0.00524	0.0584
PEM HP	0.00556	0.0095
PEM LP	0.00572	0.0638

The hydrogen production rate is independent of stack size, as larger stacks are not more energetically efficient at converting hydrogen. They use the same polarization curve, and so perform with the same efficiency for a given loading level. The production rate is also independent of stack size, as doubling the number of stacks at the same loading level will simply double the hydrogen production rate. The low-pressure designs have a higher hydrogen production rate than high pressure designs, as high pressure inhibits the reaction and lowers the efficiency of the stack. Further, PEM designs have a higher hydrogen production rate than AWE for a given load. PEM electrolyzers generally have better efficiency and polarization curve than alkaline electrolyzer stacks due to fundamental technology differences.

The balance of plant power consumption is generally independent of stack size and number of stacks as both simply increase either the water flow rate or the hydrogen (and oxygen) flow rates. The balance of plant components are entirely dependent on the flow rates of these products and reactants for their power usage, therefore when the flow rates go up, the power consumption goes up commensurately. The low-pressure designs have a considerably higher balance of plant power consumption, as they require the use of compressors to compress the hydrogen (and oxygen) to delivery pressure. This is energetically expensive compared to pumping the inlet water to the required pressure for the high-pressure designs. PEM designs also use more power for the balance of plant than AWE designs, as they produce more hydrogen for a given loading level. This increases the flow rate, increasing the balance of plant power usage.

Interestingly, these two performance characteristics work at cross purposes. The high-pressure AWE designs have the lowest hydrogen production rate per MW of the stack, but also have the lowest balance of plant power consumption, meaning the overall block will have a lower hydrogen production rate, but may also use less total power. Similarly, the low-pressure PEM designs have the highest hydrogen production rate and the highest balance of plant power consumption, meaning the overall block will have a higher hydrogen production rate, but may use more total power.

Each optimal block design used an operational point where the current density was as high as the respective technology would support. For alkaline designs this is 1 A cm^{-2}, and for PEM designs this is 2 A cm^{-2}. This indicates that the current density which represents the optimal trade-off between efficiency and capital cost is higher than is technologically feasible.

3.2 System Design

The framework was successfully able to optimize the problem and determine an optimal design and operational strategy for the 1 GW case study under examination. The effectiveness of the Dinkelbach algorithm for optimizing a nonlinear problem can be seen in Figure 3. Each

condition converged on its optimized solution after three solution cycles. This allowed the nonlinear LCOH optimization to be solved linearly, thereby reducing complexity and potentially reducing solution time relative to a nonlinear optimization.

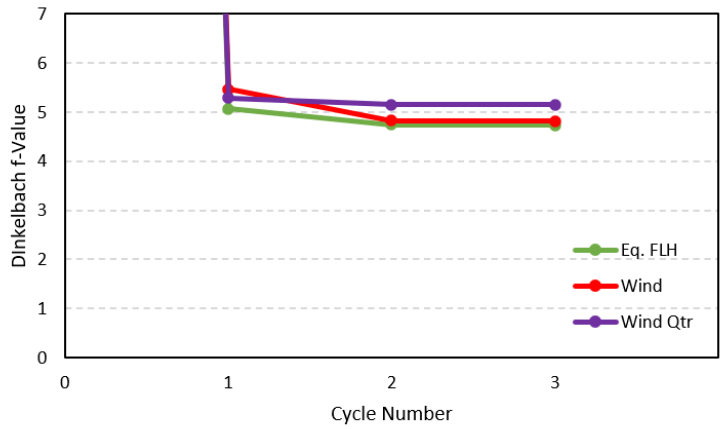

Figure 4: The convergence speed on the f-value of the Dinkelbach algorithm for each loading condition. The initial value for f, in cycle 0, was set arbitrarily high at 100 as a starting point. It is not shown on the graph to emphasize the convergence of subsequent points.

Major results of the system optimization and final system design for this case study can be found in Table 3. The equivalent full load hours loading condition has the lowest optimized levelized cost of hydrogen, at 4.73 €/kg. This loading condition has only the middle annual cost, but the highest hydrogen production rate, resulting in the lowest LCOH. The regular wind profile has the middle LCOH, despite having the lowest hydrogen production rate, because it also has the lowest annualized cost. The LCOH for the regular wind profile is only 1.9% greater than the full load hours profile, even though the hydrogen production rate is almost 6% lower due to the reduced annualized cost. The Wind Qtr load condition has the highest LCOH, a full 8.9% higher than the Eq. FLH. It has by far the highest annualized cost, but the hydrogen production rate is similar the Eq FLH condition, which is not high enough to offset the high annualized cost. These LCOH values are in the same general range as other LCOH estimates, although the scale is greater [5,27].

Table 3: The LCOH, hydrogen production quantity, and annualized cost of each optimized design.

Load Condition	LCOH (€/kg)	H_2 Prod (Mill kg/yr)	Ann. Cost (Mill €/yr)
Eq. FLH	4.73	84.4	399.6
Wind	4.82	79.6	383.8
Wind Qtr	5.15	83.2	428.3

The reason for some of these differences can be explained by the optimized designs listed in Table 4 – the specific designs will be discussed later. One major cause of differences between the various load conditions is due to the differences between AWE and PEM. PEM designs are able to ramp between different loading levels and adjust to changing loads more quickly than AWE. They are also more efficient at high current densities than AWE designs, and so can produce more hydrogen from a given amount of input power. However, PEM are more expensive to build, as noted in the previous section, and this impacts the cost of the hydrogen they can produce.

As can be seen in Table 4, the optimal design for the Eq. FLH condition introduces some PEM blocks to a design of mostly AWE blocks. This allows those few PEM blocks to produce hydrogen at a high rate using a high current density, and high efficiency. They carry most of

the power load, and the rest of the load is distributed among the remaining AWE blocks. PEM stacks are an economical choice when they are under a high, regular load. Comparing the second loading case of Wind, however, the AWE blocks are more economical when the load varies significantly. In this case, PEM blocks would not have a base load to use to produce large quantities of hydrogen, and so it is more economical to use the AWE blocks. The smaller 50 MW blocks (AWE HP 10 MW, 5 Stacks) included in the optimal design provide increased flexibility when dealing with the power swings that happen with the wind profile. Interestingly, they mostly act as a baseload plant, which is at the minimum loading level most of the time, unless the system load reaches above 915 MW, in which case they uptake the remaining load. This allows the system to keep the average load across all blocks as low as possible, where the blocks are most efficient. The accelerated wind profile, Wind Qtr, has the most complicated optimal design. The majority of the blocks are PEM, which are necessary to respond to the rapidly changing loading level. PEM block designs have a higher ramping rate than AWE designs and are necessary to take advantage the rapid power fluctuations that happen in this power profile. A larger of the two AWE block is included to act as a base load producer. The two smaller blocks, one PEM and one AWE, again provide increased flexibility in dealing with the power fluctuations.

Table 4: The final design selection, CapEx, and OpEx of each optimized design.

Load Cond.	Design Config	CapEx (Mill €)	OpEx (Mill € / yr)
Eq. FLH	AWE HP 10 MW, 10 Stacks – 7 blocks PEM HP 10MW, 10 Stacks – 3 blocks	1535	166.7
Wind	AWE HP 10 MW, 10 Stacks – 9 blocks AWE HP 10 MW, 5 Stacks – 2 blocks	1462	166.7
Wind Qtr	AWE HP 10 MW, 10 Stacks – 1 block AWE HP 10 MW, 5 Stacks – 1 block PEM HP 10 MW, 10 Stacks – 8 blocks PEM HP 10 MW, 5 Stacks – 1 block	1671	165.9

The CapEx values for the optimal designs are a direct result of the optimal design configuration. PEM blocks are more expensive than AWE blocks, and so raise the price of the total system. Larger blocks are also cheaper per MW than smaller blocks are, as a function of scale and size. The Eq. FLH load condition has a high CapEx than the Wind load condition because it uses several PEM blocks, even though the Wind load condition uses two smaller blocks, as the PEM blocks are far more expensive. The Wind Qtr load condition has the highest CapEx as the optimal design has even more PEM blocks than the Eq. FLH load condition. The OpEx result is interesting, as this is the result of the total amount of energy the system used over the year, which can be seen in Table 5. The Eq. FLH and the Wind loading conditions used the same amount of energy over the year, and so they have the same OpEx, but the OpEx is lower for the Wind Qtr load condition. This is because the system does not use all the power that is available under certain circumstances.

Table 5: The total energy used, and utilization factor of each optimized design.

Load Condition	System Energy Use, Y (GWh)	Utilization Factor
Eq. FLH	3,920	1.0
Wind	3,920	1.0
Wind Qtr	3,900	0.995

All energy available for use was used by both the Eq. FLH and the Wind load conditions, as their utilization factors are 1 for both, and the total system energy usage is the same. The Wind Qtr condition uses not all energy available under some conditions. Specifically, the

optimization occasionally chooses not to use the AWE electrolyzers during some short periods of increased wind activity. This may be a choice due a variety of factors, such as efficiency concerns or ramping rates. However, the system still uses 99.5% of the available energy, indicating this is only a problem in very limited circumstances.

4.0 Conclusions

In this work, a framework for the design and operation of a large-scale hydrogen electrolyzer has been developed and discussed. The framework takes the form of a two-part optimization problem. The first part optimizes the designs of relatively small modular units of stack and some balance of plant components, called blocks. The second part optimizes the selection of those blocks and their operational modes over the horizon of the optimization. The second part also uses the Dinkelbach algorithm, which converged on a solution within 3 cycles, as can be seen in Figure 4.

To evaluate the framework, it was applied to a case study of a 1 gigawatt, wind-powered electrolyzer based in the Netherlands, with the goal of minimizing the levelized cost of hydrogen. The case study examined alkaline water electrolysis and polymer electrolyte membrane technologies, operating at ambient pressure or at delivery pressure, stacks that are 1 MW, 5 MW, or 10 MW, and 1, 5, or 10 stacks per block. It also looked at three different power supply profiles, where the first profile was a constant power supply, the second was the power production profile of a theoretical 1 GW plant off the coast of the Netherlands, and the third profile was an accelerated wind profile. These different wind profiles were used to demonstrate how it can impact the design choices made by the optimization.

Using the framework to optimize the design and operation of the electrolyzer plant for this case study found that there were differences in the design, levelized cost of hydrogen, and operation of the plant for the different power supply scenarios. The optimization found that for this case study AWE designs are cheaper than equivalent PEM designs, and that larger blocks are cheaper than smaller blocks per MW. Of the scenarios examined, the constant power supply condition resulted in the most hydrogen being produced, 84.4 million kg as seen in Table 3, and lowest levelized cost of hydrogen, at 4.73 €/kg. The wind power condition produced the least hydrogen out of the three power profiles, at 79.6 million kg, but only increased the levelized cost of hydrogen by 2% to 4.82 €/kg due to savings in cost from a different design, which can be seen in Table 4. Generally speaking, fast moving power profiles like the accelerated wind profile, Wind Qtr, used more PEM technology designs, as they are able to more quickly respond to changes in loading level, which is beneficial despite being the highest capital cost, at 1671 million €. However, the framework still chose to have a mix of technology types, indicating a potential benefit to technology mixing. It is important to state that when using power sources that shift more rapidly, the use of PEM electrolyzers will rise, as their increased ramping rates are more impactful.

The framework developed in this work is a useful tool for designers of large-scale electrolysis plants. It offers the ability to rapidly understand the impact of various design options, and how the optimal design could be impacted by changes in various inputs. These types of plants are of interest to those who are in the hydrogen industry, and those who want to encourage the renewable feedstock industry. This framework may also be useful for large scale designs of other electrochemical systems provided the appropriate inputs.

Acknowledgements
This research was carried out in the context of the ‘Hydrohub Gigawatt Scale Electrolyzer’ project, coordinated by the Institute for Sustainable Process Technology (ISPT) and co-funded by TKI-E&I with the supplementary grant 'TKI- Toeslag' for Topconsortia for Knowledge and Innovation (TKI’s) of the Ministry of Economic Affairs and Climate Policy.

Conflicts of Interest
There are no conflicts of interest to declare.

References

[1] A Roadmap for moving to a competitive low carbon economy in 2050. vol. 34. Brussels, Belgium: 2011. https://doi.org/10.1002/jsc.572.

[2] Department for Business Energy and Industrial Strategy. Explanatory Memorandum To the Climate Change Act 2008 (2050 Target Amendment) Order 2019. LegislationGovUk 2019:4.

[3] International Energy Agency. The Future of Hydrogen. 2019. https://doi.org/10.1016/S1464-2859(12)70027-5.

[4] Zeng K, Zhang D. Recent progress in alkaline water electrolysis for hydrogen production and applications. Prog Energy Combust Sci 2010;36:307–26. https://doi.org/10.1016/j.pecs.2009.11.002.

[5] Loisel R, Baranger L, Chemouri N, Spinu S, Pardo S. Economic evaluation of hybrid off-shore wind power and hydrogen storage system. Int J Hydrogen Energy 2015;40:6727–39. https://doi.org/10.1016/j.ijhydene.2015.03.117.

[6] Schiebahn S, Grube T, Robinius M, Tietze V, Kumar B, Stolten D. Power to gas: Technological overview, systems analysis and economic assessment for a case study in Germany. Int J Hydrogen Energy 2015;40:4285–94. https://doi.org/10.1016/j.ijhydene.2015.01.123.

[7] Walker SB, Van Lanen D, Fowler M, Mukherjee U. Economic analysis with respect to Power-to-Gas energy storage with consideration of various market mechanisms. Int J Hydrogen Energy 2016;41:7754–65. https://doi.org/10.1016/j.ijhydene.2015.12.214.

[8] Saur G, Ramsden T. Wind Electrolysis : Hydrogen Cost Optimization. Golden, CO: 2011.

[9] Troncoso E, Newborough M. Electrolysers for mitigating wind curtailment and producing "green" merchant hydrogen. Int J Hydrogen Energy 2011;36:120–34. https://doi.org/10.1016/j.ijhydene.2010.10.047.

[10] Rahil A, Gammon R, Brown N. Flexible operation of electrolyser at the garage forecourt to support grid balancing and exploitation of hydrogen as a clean fuel. Res Transp Econ 2018;70:125–38. https://doi.org/10.1016/j.retrec.2017.12.001.

[11] Zhang X, Chan SH, Ho HK, Tan SC, Li M, Li G, et al. Towards a smart energy network: The roles of fuel/electrolysis cells and technological perspectives. Int J Hydrogen Energy 2015;40:6866–919. https://doi.org/10.1016/j.ijhydene.2015.03.133.

[12] Schmidt O, Gambhir A, Staffell I, Hawkes A, Nelson J, Few S. Future cost and performance of water electrolysis: An expert elicitation study. Int J Hydrogen Energy 2017;42:30470–92. https://doi.org/10.1016/j.ijhydene.2017.10.045.

[13] Marini S, Salvi P, Nelli P, Pesenti R, Villa M, Berrettoni M, et al. Advanced alkaline water electrolysis. Electrochim Acta 2012;82:384–91. https://doi.org/10.1016/j.electacta.2012.05.011.

[14] Lee B, Cho HS, Kim H, Lim D, Cho W, Kim CH, et al. Integrative techno-economic and environmental assessment for green H2 production by alkaline water electrolysis based on experimental data. J Environ Chem Eng 2021;9:106349. https://doi.org/10.1016/j.jece.2021.106349.

[15] Carmo M, Fritz DL, Mergel J, Stolten D. A comprehensive review on PEM water electrolysis. Int J Hydrogen Energy 2013;38:4901–34. https://doi.org/10.1016/j.ijhydene.2013.01.151.

[16] El-Emam RS, Özcan H. Comprehensive review on the techno-economics of sustainable large-scale clean hydrogen production. J Clean Prod 2019;220:593–609. https://doi.org/10.1016/j.jclepro.2019.01.309.

[17] Cai Q, Luna-Ortiz E, Adjiman CS, Brandon NP. The effects of operating conditions on the performance of a solid oxide steam electrolyser: A model-based study. Fuel Cells 2010;10:1114–28. https://doi.org/10.1002/fuce.200900211.

[18] Jørgensen C, Ropenus S. Production price of hydrogen from grid connected electrolysis in a power market with high wind penetration. Int J Hydrogen Energy 2008;33:5335–44. https://doi.org/10.1016/j.ijhydene.2008.06.037.

[19] Zhang G, Wan X. A wind-hydrogen energy storage system model for massive wind energy curtailment. Int J Hydrogen Energy 2014;39:1243–52.

https://doi.org/10.1016/j.ijhydene.2013.11.003.
[20] Green R, Hu H, Vasilakos N. Turning the wind into hydrogen: The long-run impact on electricity prices and generating capacity. Energy Policy 2011;39:3992–8. https://doi.org/10.1016/j.enpol.2010.11.007.
[21] Bennoua S, Le Duigou A, Quéméré MM, Dautremont S. Role of hydrogen in resolving electricity grid issues. Int J Hydrogen Energy 2015;40:7231–45. https://doi.org/10.1016/j.ijhydene.2015.03.137.
[22] Grueger F, Möhrke F, Robinius M, Stolten D. Early power to gas applications: Reducing wind farm forecast errors and providing secondary control reserve. Appl Energy 2017;192:551–62. https://doi.org/10.1016/j.apenergy.2016.06.131.
[23] Chang PL, Hsu CW, Hsiung CM. Functional assessment for large-scale wind-hydrogen energy integration electricity supply system in Taiwan. IEEE Int Conf Ind Eng Eng Manag 2014:1283–7. https://doi.org/10.1109/IEEM.2013.6962617.
[24] Menanteau P, Quéméré MM, Le Duigou A, Le Bastard S. An economic analysis of the production of hydrogen from wind-generated electricity for use in transport applications. Energy Policy 2011;39:2957–65. https://doi.org/10.1016/j.enpol.2011.03.005.
[25] Dagdougui H, Ouammi A, Sacile R. Modelling and control of hydrogen and energy flows in a network of green hydrogen refuelling stations powered by mixed renewable energy systems. Int J Hydrogen Energy 2012;37:5360–71. https://doi.org/10.1016/j.ijhydene.2011.07.096.
[26] Kim J, Lee H, Lee B, Kim J, Oh H, Lee IB, et al. An integrative process of blast furnace and SOEC for hydrogen utilization: Techno-economic and environmental impact assessment. Energy Convers Manag 2021;250:114922. https://doi.org/10.1016/j.enconman.2021.114922.
[27] Lee B, Chae H, Choi NH, Moon C, Moon S, Lim H. Economic evaluation with sensitivity and profitability analysis for hydrogen production from water electrolysis in Korea. Int J Hydrogen Energy 2017;42:6462–71. https://doi.org/10.1016/j.ijhydene.2016.12.153.
[28] Yates J, Daiyan R, Patterson R, Egan R, Amal R, Ho-Baille A, et al. Techno-economic Analysis of Hydrogen Electrolysis from Off-Grid Stand-Alone Photovoltaics Incorporating Uncertainty Analysis. Cell Reports Phys Sci 2020;1:100209. https://doi.org/10.1016/j.xcrp.2020.100209.
[29] Gallardo FI, Monforti Ferrario A, Lamagna M, Bocci E, Astiaso Garcia D, Baeza-Jeria TE. A Techno-Economic Analysis of solar hydrogen production by electrolysis in the north of Chile and the case of exportation from Atacama Desert to Japan. Int J Hydrogen Energy 2021;46:13709–28. https://doi.org/10.1016/j.ijhydene.2020.07.050.
[30] Sadeghi S, Ghandehariun S, Rosen MA. Comparative economic and life cycle assessment of solar-based hydrogen production for oil and gas industries. Energy 2020;208:118347. https://doi.org/10.1016/j.energy.2020.118347.
[31] Böhm H, Zauner A, Rosenfeld DC, Tichler R. Projecting cost development for future large-scale power-to-gas implementations by scaling effects. Appl Energy 2020;264:114780. https://doi.org/10.1016/j.apenergy.2020.114780.
[32] Turton R, Bailie R, Whiting W, Shaeiwitz J, Bhattacharyya D. Analysis, Synthesis, and Design of Chemical Processes. 3rd Editio. Upper Sale River, NJ: Prentice Hall; 2009.
[33] Bejan A, Tsatsaronis G, Moran MJ. Thermal Design and Optimization. New York and Chichester: John Wiley; 1996.
[34] Pierobon L, Nguyen T Van, Larsen U, Haglind F, Elmegaard B. Multi-objective optimization of organic Rankine cycles for waste heat recovery: Application in an offshore platform. Energy 2013;58:538–49. https://doi.org/10.1016/j.energy.2013.05.039.
[35] Olivier P, Bourasseau C, Bouamama PB. Low-temperature electrolysis system modelling: A review. Renew Sustain Energy Rev 2017;78:280–300. https://doi.org/10.1016/j.rser.2017.03.099.
[36] Buttler A, Spliethoff H. Current status of water electrolysis for energy storage, grid balancing and sector coupling via power-to-gas and power-to-liquids: A review. Renew Sustain Energy Rev 2018;82:2440–54. https://doi.org/10.1016/j.rser.2017.09.003.
[37] Ulleberg Ø. Modeling of advanced alkaline electrolyzers: A system simulation approach. Int J Hydrogen Energy 2003;28:21–33. https://doi.org/10.1016/S0360-3199(02)00033-2.
[38] García-Valverde R, Espinosa N, Urbina A. Optimized method for photovoltaic-water

electrolyser direct coupling. Int J Hydrogen Energy 2011;36:10574–86. https://doi.org/10.1016/j.ijhydene.2011.05.179.
[39] García-Valverde R, Espinosa N, Urbina A. Simple PEM water electrolyser model and experimental validation. Int J Hydrogen Energy 2012;37:1927–38. https://doi.org/10.1016/j.ijhydene.2011.09.027.
[40] Bensmann B, Hanke-Rauschenbach R, Peña Arias IK, Sundmacher K. Energetic evaluation of high pressure PEM electrolyzer systems for intermediate storage of renewable energies. Electrochim Acta 2013;110:570–80. https://doi.org/10.1016/j.electacta.2013.05.102.
[41] Parks G, Boyd R, Cornish J, Remick R. Hydrogen Station Compression, Storage, and Dispensing Technical Status and Costs: Systems Integration. Golden, CO: 2014.
[42] Heberle F, Brüggemann D. Thermo-economic analysis of zeotropic mixtures and pure working fluids in Organic Rankine Cycles for waste heat recovery. Energies 2016;9. https://doi.org/10.3390/en9040226.
[43] Minutillo M, Perna A, Forcina A, Di Micco S, Jannelli E. Analyzing the levelized cost of hydrogen in refueling stations with on-site hydrogen production via water electrolysis in the Italian scenario. Int J Hydrogen Energy 2021;46:13667–77. https://doi.org/10.1016/j.ijhydene.2020.11.110.
[44] Liu S, Simaria AS, Farid SS, Papageorgiou LG. Optimising chromatography strategies of antibody purification processes by mixed integer fractional programming techniques. Comput Chem Eng 2014;68:151–64. https://doi.org/10.1016/j.compchemeng.2014.05.005.
[45] Dinkelbach W. On Nonlinear Fractional Programming. Manage Sci 1967;13:492–8. https://doi.org/10.1287/mnsc.13.7.492.
[46] Mostafa MH, Abdel Aleem SHE, Ali SG, Ali ZM, Abdelaziz AY. Techno-economic assessment of energy storage systems using annualized life cycle cost of storage (LCCOS) and levelized cost of energy (LCOE) metrics. J Energy Storage 2020;29:101345. https://doi.org/10.1016/j.est.2020.101345.
[47] ISPT. Hydrohub Gigawatt Scale Electrolyser 2018. https://ispt.eu/projects/hydrohub-gigawatt/.
[48] Pfenninger S, Staffell I. Renewables.ninja n.d. https://www.renewables.ninja/ (accessed November 1, 2019).
[49] Pfenninger S, Staffell I. Long-term patterns of European PV output using 30 years of validated hourly reanalysis and satellite data. Energy 2016;114:1251–65. https://doi.org/10.1016/j.energy.2016.08.060.
[50] Staffell I, Pfenninger S. Using bias-corrected reanalysis to simulate current and future wind power output. Energy 2016;114:1224–39. https://doi.org/10.1016/j.energy.2016.08.068.
[51] Green Hydrogen Cost Reduction: Scaling up electrolysers to meet the 1.5 C climate goal. Abu Dhabi: IRENA; 2020.
[52] thyssenkrupp Uhde Chlorine Engineers. Hydrogen from Large-Scale Electrolysis 2018.
[53] Centrifugal vs. reciprocating compressors. Turbomach Int 2016. https://www.turbomachinerymag.com/view/centrifugal-vs-reciprocating-compressor.
[54] Jenkins S. CEPCI Updates: January 2018 (prelim.) and December 2017 (final). Chem Eng 2018.
[55] Krishnan S, Fairlie M, Andres P, De Groot T, Kramer GJ. Power to gas (H2): Alkaline electrolysis. Technol Learn Transit to a Low-Carbon Energy Syst Concept Issues, Empir Find Use, Energy Model 2019:165–87. https://doi.org/10.1016/B978-0-12-818762-3.00010-8.
[56] Abdin Z, Webb CJ, Gray EM. Modelling and simulation of a proton exchange membrane (PEM) electrolyser cell. Int J Hydrogen Energy 2015;40:13243–57. https://doi.org/10.1016/j.ijhydene.2015.07.129.
[57] Diéguez PM, Ursúa A, Sanchis P, Sopena C, Guelbenzu E, Gandía LM. Thermal performance of a commercial alkaline water electrolyzer: Experimental study and mathematical modeling. Int J Hydrogen Energy 2008;33:7338–54. https://doi.org/10.1016/j.ijhydene.2008.09.051.
[58] Parra D, Patel MK. Techno-economic implications of the electrolyser technology and size for power-to-gas systems. Int J Hydrogen Energy 2016;41:3748–61. https://doi.org/10.1016/j.ijhydene.2015.12.160.
[59] Jansen M, Staffell I, Kitzing L, Quoilin S, Wiggelinkhuizen E, Bulder B, et al. Offshore wind competitiveness in mature markets without subsidy. Nat Energy 2020;5:614–22.

https://doi.org/10.1038/s41560-020-0661-2.
[60] IRENA. Renewable energy auctions. vol. 1. 2017.